

AUTOMATED GRAPH SELF-SUPERVISED LEARNING VIA MULTI-TEACHER KNOWLEDGE DISTILLATION

Lirong Wu, Yufei Huang, Haitao Lin, Zicheng Liu, Tianyu Fan, and Stan Z. Li

AI Lab, School of Engineering, Westlake University

{wulirong, huangyufei, linhaitao, stan.zq.li}@westlake.edu.cn

ABSTRACT

Self-supervised learning on graphs has recently achieved remarkable success in graph representation learning. With hundreds of self-supervised pretext tasks proposed over the past few years, the research community has greatly developed, and the key is no longer to design more powerful but complex pretext tasks, but to make more effective use of those already on hand. This paper studies the problem of how to automatically, adaptively, and dynamically learn instance-level self-supervised learning strategies for each node from a given pool of pretext tasks. In this paper, we propose a novel multi-teacher knowledge distillation framework for Automated Graph Self-Supervised Learning (AGSSL), which consists of two main branches: (i) *Knowledge Extraction*: training multiple teachers with different pretext tasks, so as to extract different levels of knowledge with different inductive biases; (ii) *Knowledge Integration*: integrating different levels of knowledge and distilling them into the student model. Without simply treating different teachers as equally important, we provide a provable theoretical guideline for how to integrate the knowledge of different teachers, i.e., the integrated teacher probability should be close to the true Bayesian class-probability. To approach the theoretical optimum in practice, two adaptive knowledge integration strategies are proposed to construct a relatively “good” integrated teacher. Extensive experiments on eight datasets show that AGSSL can benefit from multiple pretext tasks, outperforming the corresponding individual tasks; by combining a few simple but classical pretext tasks, the resulting performance is comparable to other leading counterparts.

1 INTRODUCTION

Deep learning on graphs (Hamilton et al., 2017; Kipf & Welling, 2016; Veličković et al., 2017; Wu et al., 2020) has recently achieved remarkable success on a variety of tasks, while such success relies heavily on the massive and carefully labeled data. However, precise annotations are usually very expensive and time-consuming. Recent advances in graph *Self-supervised Learning* (SSL) (Wu et al., 2021; Xie et al., 2021; Liu et al., 2021) have provided novel insights into reducing the dependency on annotated labels and enable the training on massive unlabeled data. The primary goal of graph SSL is to provide self-supervision for learning transferable knowledge from abundant unlabeled data, through well-designed pretext tasks (in the form of loss functions). There have been hundreds of pretext tasks proposed in the past few years (Sun et al., 2019; Hu et al., 2019; Xia et al., 2022; 2021; Zhu et al., 2020a; You et al., 2020a; Zhang et al., 2020), and different pretext tasks extract different levels of graph knowledge based on different inductive biases. For example, PAIRDIS (Jin et al., 2020) captures the inter-node long-range dependencies by predicting the shortest path lengths between nodes, while PAR (You et al., 2020b) extracts topological information by predicting the graph partitions of nodes. With so many ready-to-use pretext tasks already on hand, as opposed to designing more complex pretext tasks (for minor performance gains), a more promising problem is *how to automatically, adaptively, and dynamically leverage multiple existing pretext tasks effectively*.

The investigations on five self-supervised pretext tasks, including PAR, CLU (You et al., 2020b), DGI (Veličković et al., 2019), PAIRDIS and PAIRSIM (Jin et al., 2020), yielded some interesting observations, from which we identify three main challenges for automated graph SSL: (i) *Dataset-level dependency*. The node classification performance rankings in Fig. 1(a) indicate that different pretext tasks have distinct downstream performance across eight datasets, and the success of pretext tasks strongly depends on the dataset characteristics. (ii) *Task-level compatibility*. The results reported in Fig. 1(b) are quite counterintuitive, where learning representations with multiple pretext tasks does

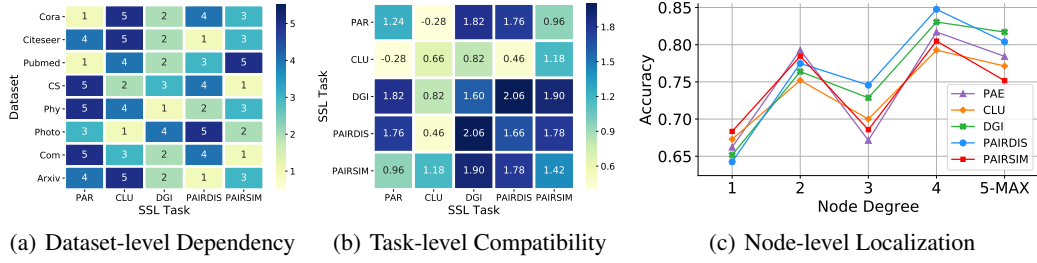


Figure 1: **(a)** Performance ranking (1: best, 5: poorest) of different pretext tasks on eight datasets. **(b)** Performance gains or drops over the vanilla GCNs on *Citeseer* when combining two tasks. **(c)** Classification accuracy of nodes with different node degrees across five pretext tasks on *Citeseer*.

not necessarily lead to better performance, because pretext tasks involving different inductive biases may be incompatible with each other. *(iii) Node-level Localization.* We present the classification accuracy of nodes with different node degrees across five pretext tasks in Fig. 1(c), from which we observe that different nodes may require localized pretext tasks; for example, high-degree nodes benefit more from DGI and PAIRDIS, while low-degree nodes prefer CLU and PAIRSIM.

Given an unseen graph dataset and a pool of pre-given pretext tasks, this paper aims to design an automated graph self-supervised learning framework that meets the following four desirable properties: *(i) automated*, completely free of human labor or trial-and-error on pretext task choices; *(ii) adaptive*, generalizing well to various graph datasets; *(iii) dynamic*, allowing for different types of pretext tasks at different training stages; *(iv) localized*, learning a customized combination of pretext tasks for each node separately and providing instance-level explanations on the importance of different tasks for each node. Compared to previous hand-crafted, dataset-specific task selection, this paper achieves an unprecedented degree of flexibility. We summarize our contributions as

- We propose a novel multi-teacher knowledge distillation framework for Automated Graph Self-Supervised Learning (AGSSL), which can automatically, adaptively, and dynamically learn instance-level self-supervised learning strategies for each node separately.
- We provide a provable theoretical guideline for how to integrate the knowledge of different teachers, i.e., the integrated teacher probability should be close to the true class-Bayesian probability. Moreover, we prove theoretically that the optimal integrated teacher probability can monotonically approach the Bayesian class-probability as the number of teachers increases.
- Two knowledge integration strategies are proposed to construct a relatively “good” teacher by adaptively adjusting the weights of different knowledge for each node during distillation.
- Extensive experiments on eight datasets demonstrate that AGSSL can benefit from multiple pretext tasks and significantly improve the performance of individual tasks. By combining only a few simple pretext tasks, the resulting performance is comparable to other leading counterparts.

2 PRELIMINARIES

Notations. Let $\mathcal{G} = (\mathcal{V}, \mathcal{E}, \mathbf{X})$ denote an attributed graph, where \mathcal{V} is the set of $|\mathcal{V}| = N$ nodes with features $\mathbf{X} = [\mathbf{x}_1, \mathbf{x}_2, \dots, \mathbf{x}_N] \in \mathbb{R}^{N \times d}$ and $\mathcal{E} \subseteq \mathcal{V} \times \mathcal{V}$ is the set of $|\mathcal{E}|$ edges between nodes. Following the common semi-supervised node classification setting, only a subset of node $\mathcal{V}_L = \{v_1, v_2, \dots, v_L\}$ with corresponding labels $\mathcal{Y}_L = \{y_1, y_2, \dots, y_L\}$ are known, and we denote the labeled set as $\mathcal{D}_L = (\mathcal{V}_L, \mathcal{Y}_L)$ and unlabeled set as $\mathcal{D}_U = (\mathcal{V}_U, \mathcal{Y}_U)$, where $\mathcal{V}_U = \mathcal{V} \setminus \mathcal{V}_L$. The task of node classification aims to learn a GNN encoder $f_\theta(\cdot)$ and a linear prediction head $g_\omega(\cdot)$ with the task loss $\mathcal{L}_{\text{task}}(\theta, \omega)$ on labeled data \mathcal{D}_L , so that they can be used to infer the labels \mathcal{Y}_U .

Problem Statement. Given a GNN encoder $f_\theta(\cdot)$, a linear prediction head $g_\omega(\cdot)$, and a set of K self-supervised losses $\{\mathcal{L}_{\text{ssl}}^{(1)}(\theta, \eta_1), \mathcal{L}_{\text{ssl}}^{(2)}(\theta, \eta_2), \dots, \mathcal{L}_{\text{ssl}}^{(K)}(\theta, \eta_K)\}$ with prediction heads $\{g_{\eta_k}(\cdot)\}_{k=1}^K$, two common strategies for combining self-supervised losses $\{\mathcal{L}_{\text{ssl}}^{(k)}(\theta, \eta_k)\}_{k=1}^K$ and semi-supervised loss $\mathcal{L}_{\text{task}}(\theta, \omega)$ are *Joint Training* (JT) and *Pre-train&Fine-tune* (P&F), as shown in Fig. 2. The *Joint Training* strategy jointly train the entire model under the supervision of downstream task and pretext tasks, which can be considered as a kind of multi-task learning, defined as

$$\theta^*, \omega^*, \{\eta_k^*\}_{k=1}^K = \arg \min_{\theta, \omega, \{\eta_k\}_{k=1}^K} \mathcal{L}_{\text{task}}(\theta, \omega) + \alpha \sum_{k=1}^K \lambda_k \mathcal{L}_{\text{ssl}}^{(k)}(\theta, \eta_k) \quad (1)$$

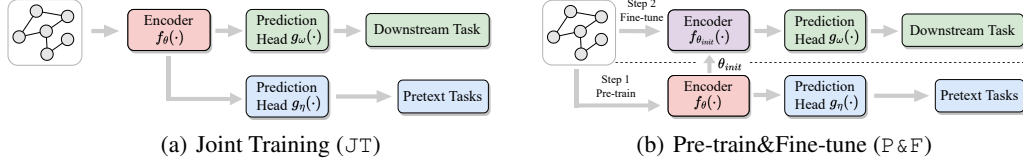


Figure 2: Illustration of the two training strategies, namely Joint Training and Pre-train&Fine-tune.

where α is a trade-off hyperparameter and $\{\lambda_k\}_{k=1}^K$ are task weights. The *Pre-train&Fine-tune* strategy works in a two-stage manner: (1) Pre-training the GNN encoder $f_\theta(\cdot)$ with self-supervised pretext tasks; and (2) Fine-tuning the pre-trained GNN encoder $f_{\theta_{init}}(\cdot)$ with a prediction head $g_\omega(\cdot)$ under the supervision of a specific downstream task. The learning objective can be formulated as

$$\theta^*, \omega^* = \arg \min_{(\theta, \omega)} \mathcal{L}_{\text{task}}(\theta_{init}, \omega), \quad \text{s.t.} \quad \theta_{init}, \{\eta_k^*\}_{k=1}^K = \arg \min_{\theta, \{\eta_k\}_{k=1}^K} \sum_{k=1}^K \lambda_k \mathcal{L}_{\text{ssl}}^{(k)}(\theta, \eta_k) \quad (2)$$

A high-level overview of the two strategies is shown in Fig. 2. Without loss of generality, we mainly introduce our framework for the JT strategy, leaving extensions to the P & F strategy in **Appendix A**.

Graph Self-supervised Learning Automation. A Vanilla solution to combine multiple self-supervised pretext tasks is to set the task weight $\lambda_k = \frac{1}{K}$ ($1 \leq k \leq K$), i.e., to treat different tasks as equally important, but this completely conflicts with the observations from Fig. 1. Furthermore, the experimental results in Table. 1 also show that the performance of simply averaging over different tasks may not only fail to match the performance of individual tasks, but may even be inferior to the vanilla implementation without any pretext tasks. Different from hand-crafted task weight settings, AutoSSL (Jin et al., 2021) proposes to learn a set of task weights $\{\lambda_k\}_{k=1}^K$ such that $f_\theta(\cdot)$ trained with the weighted loss $\sum_{k=1}^K \lambda_k \mathcal{L}_{\text{ssl}}^{(k)}(\theta, \eta_k)$ can extract meaningful representations. Specifically, AutoSSL formulates the automated self-supervised task search as a bi-level optimization problem and solves it via meta-gradient descent (Finn et al., 2017; Zügner & Günnemann, 2019), as follows

$$\min_{\{\lambda_k\}_{k=1}^K} \mathcal{H}(f_{\theta^*}(\mathcal{G})), \quad \text{s.t.} \quad \theta^*, \omega^*, \{\eta_k^*\}_{k=1}^K = \arg \min_{\theta, \omega, \{\eta_k\}_{k=1}^K} \mathcal{L}_{\text{task}}(\theta, \omega) + \alpha \sum_{k=1}^K \lambda_k \mathcal{L}_{\text{ssl}}^{(k)}(\theta, \eta_k) \quad (3)$$

where $\mathcal{H}(\cdot)$ denotes the quality measure of the node representations $f_{\theta^*}(\mathcal{G})$, and it can be any metric that evaluates the downstream performance, such as the cross-entropy loss on the labeled data \mathcal{V}_L for the semi-supervised learning setting. In practice, how to define $\mathcal{H}(\cdot)$ is usually a heuristic problem that requires a lot of manual labor, which may not satisfy the “automated” condition. Secondly, adjusting task weights can alleviate, but not completely solve, the task-level compatibility problem, because the loss of a task with small weight can still couple with and affect other tasks (Kendall et al., 2018; Chen et al., 2018). Thirdly, the learned task weights may fail to explain the importance of different tasks, since the weights of different self-supervised losses can be of different orders of magnitude, and thus high-weighted losses do not necessarily dominate in optimization. Last but not least, AutoSSL only learns **global** task weights for each dataset, but completely ignores the node-level localization (as found in Fig. 1(c)). Considering these four limitations, we propose a novel multi-teacher knowledge distillation framework for **Automated Graph Self-Supervised Learning** (AGSSL), which can learn instance-level self-supervised strategies for each node separately.

3 METHODOLOGY

3.1 MULTI-TEACHER KNOWLEDGE DISTILLATION

Intuitively, training with multiple pretext tasks enables the model to access richer information, which is beneficial for improving performance. However, this holds true only if we can well handle the compatibility problem between pretext tasks. Previous approaches, such as AutoSSL, have attempted to jointly train multiple pretext tasks by adaptively learning global task weights, but this learning process is a black box in which multiple tasks are coupled with each other to produce unexplainable “mixed” representations. To make matters worse, this renders the training of a primary task vulnerable to other relatively unrelated tasks, leading to suboptimal results. In this paper, we propose a novel multi-teacher knowledge distillation framework - AGSSL in Fig. 3, where we train multiple teachers with different pretext tasks to extract different levels of knowledge, which are then

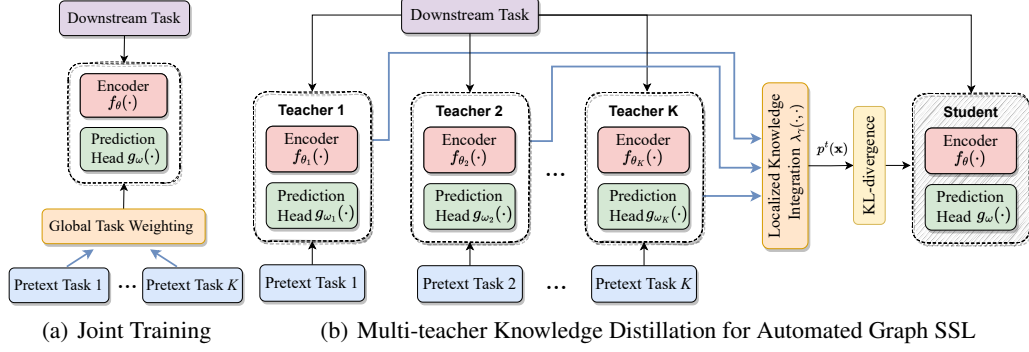


Figure 3: **(a)** Conventional multi-task self-supervised learning where the model is jointly trained with multiple (globally) weighted pretext tasks. **(b)** Proposed multi-teacher knowledge distillation framework, where we train each teacher separately with one pretext task and then apply a localized integration module to integrate different levels of knowledge and distill them into the student model.

integrated through a localized knowledge integration module $\lambda_\gamma(\cdot, \cdot)$ and finally distilled into the student model. The learning objective of AGSSL can be formulated as follows

$$\begin{aligned} \min_{\theta, \omega, \gamma} \mathcal{L}_{\text{task}}(\theta, \omega) + \beta \frac{\tau^2}{N} \sum_{i=1}^N \mathcal{L}_{KL} \left(\text{softmax}(\mathbf{z}_i / \tau), \sum_{k=1}^K \lambda_\gamma(k, i) \text{softmax}(\mathbf{h}_i^{(k)} / \tau) \right) \\ \text{s.t. } \theta_k^*, \omega_k^*, \eta_k^* = \arg \min_{\theta_k, \omega_k, \eta_k} \mathcal{L}_{\text{task}}(\theta_k, \omega_k) + \alpha \mathcal{L}_{\text{ssl}}^{(k)}(\theta_k, \eta_k), \text{ where } 1 \leq k \leq K \end{aligned} \quad (4)$$

where $\mathbf{z}_i = g_\omega(f_\theta(\mathcal{G}, i))$ and $\mathbf{h}_i^{(k)} = g_{\omega_k^*}(f_{\theta_k^*}(\mathcal{G}, i))$ are the logits of node v_i in the student model and k -th teacher model, respectively. Besides, $\mathcal{L}_{KL}(\cdot, \cdot)$ denotes the KL-divergence loss, and $\lambda_\gamma(k, i)$ is a weighting function that outputs the importance weight of k -th pretext task for node v_i , which satisfies $\sum_{k=1}^K \lambda_\gamma(k, i) = 1$. In addition, β is a trade-off hyperparameter, τ is the distillation temperature, and τ^2 is used to keep the gradient stability of this loss. The knowledge distillation is first introduced in (Hinton et al., 2015), where knowledge is transferred from a cumbersome teacher to a lightweight student. In this paper, not to get a simpler student model, we adopt the multi-teacher knowledge distillation framework to **automatically**, **adaptively**, and **dynamically** distill different levels of knowledge into one student model. Besides, AGSSL takes full account of the node-level **localization** and learns a customized knowledge integration strategy for each node through a parameterized function $\lambda_\gamma(\cdot, \cdot)$. Moreover, since the knowledge extracted by different tasks is mapped into the same probability space and the node-level weights satisfy $\sum_{k=1}^K \lambda_\gamma(k, i) = 1$, the weight $\lambda_\gamma(k, i)$ can more truly **explain** the importance of k -th pretext task to node v_i .

3.2 THEORETICAL GUIDELINE FOR HOW TO INTEGRATE

One more problem left to be solved in Sec. 3.1 is how to integrate different levels of knowledge, that is, how to design and learn a suitable knowledge weighting function $\lambda_\gamma(k, i)$. In this section, we (P1) establish a provable theoretical guideline that tells us how to integrate, i.e., *what is the criteria for constructing a relatively “good” integrated teacher*; (P2) a theory-guided practical implementation; and (P3) a theoretical justification for the advantages of AGSSL under the multi-task learning setting.

(P1) Let us define $R(\theta, \omega) = \mathbb{E}_{\mathbf{x}} [\mathbb{E}_{y|\mathbf{x}} [\ell(y, \text{softmax}(g_\omega(f_\theta(\mathbf{x}))/\tau))]] = \mathbb{E}_{\mathbf{x}} [\mathbf{p}^*(\mathbf{x})^\top \mathbf{l}(g_\omega(f_\theta(\mathbf{x})))]$ as **Bayesian objective**, where $\mathbf{p}^*(x) \doteq [\mathbb{P}(y|x)]_{y \in [C]}$ is defined as the Bayesian probability. $\mathbf{l}(g_\omega(f_\theta(\mathbf{x}))) = (\ell(1, \text{softmax}(g_\omega(f_\theta(\mathbf{x}))/\tau)), \dots, \ell(C, \text{softmax}(g_\omega(f_\theta(\mathbf{x}))/\tau)))$ is the loss vector, where $\ell(\cdot, \cdot)$ is the cross-entropy loss and C is the number of category. To simplify the notations, we can set $\tilde{\mathbf{z}}_i \doteq \text{softmax}(\mathbf{z}_i / \tau)$, $\tilde{\mathbf{h}}_i^{(k)} \doteq \text{softmax}(\mathbf{h}_i^{(k)} / \tau)$, and $\mathbf{p}^t(\mathbf{x}_i) \doteq \sum_{k=1}^K \lambda_\gamma(k, i) \tilde{\mathbf{h}}_i^{(k)}$, and then we can rewrite the the second distillation term of Eq. (4) as the **distillation objective**, as follows

$$\frac{1}{N} \sum_{i=1}^N \mathcal{L}_{KL} \left(\tilde{\mathbf{z}}_i, \sum_{k=1}^K \lambda_\gamma(k, i) \tilde{\mathbf{h}}_i^{(k)} \right) \propto \frac{1}{N} \sum_{i=1}^N \mathbf{p}^t(\mathbf{x}_i)^\top \mathbf{l}(g_\omega(f_\theta(\mathbf{x}_i))) \doteq \tilde{R}(\theta, \omega) \quad (5)$$

where the detailed derivation of Eq. (5) is available in **Appendix B**. Previous work (Menon et al., 2021) has provided a statistical perspective on single-teacher knowledge distillation, where

a Bayesian teacher providing true class probabilities $\{\mathbf{p}^*(\mathbf{x}_i)\}_{i=1}^N$ can lower the variance of the **downstream objective** $\mathcal{L}_{\text{task}}(\theta, \omega) = \frac{1}{N} \sum_{i=1}^N \mathbf{e}_{y_i}^T \mathbf{1}(g_\omega(f_\theta(\mathbf{x}_i)))$, where $\mathbf{e}_{y_i}^T$ is the one-hot label of node v_i ; the reward of reducing variance is beneficial for improving generalization (Maurer & Pontil, 2009). However, the teacher probabilities $\{\tilde{\mathbf{h}}_i^{(k)}\}_{k=1}^K$ and Bayesian probability $\mathbf{p}^*(\mathbf{x}_i)$ are very likely to be *linearly independent* in the multi-teacher distillation framework, which means that we cannot guarantee $\mathbf{p}^t(\mathbf{x}_i) = \sum_{k=1}^K \lambda_\gamma(k, i) \tilde{\mathbf{h}}_i^{(k)} = \mathbf{p}^*(\mathbf{x}_i)$ for node $v_i \in \mathcal{V}$ by just adjusting weights $\{\lambda_\gamma(k, i)\}_{k=1}^K$. In practice, the following Proposition 1 indicates that an imperfect teacher $\mathbf{p}^t(\mathbf{x}) \neq \mathbf{p}^*(\mathbf{x})$ can still improve generalization by approximating the Bayesian teacher $\mathbf{p}^*(\mathbf{x})$.

Proposition 1 Consider an integrated teacher $\mathbf{p}^t(\mathbf{x})$ and a Bayesian teacher $\mathbf{p}^*(\mathbf{x})$. For any GNN encoder $f_\theta(\cdot)$ and prediction head $g_\omega(\cdot)$, the difference between the distillation objective $\tilde{R}(\theta, \omega)$ and Bayesian objective $R(\theta, \omega)$ is bounded by the Mean Square Error (MSE) of their probabilities,

$$\mathbb{E} \left[\left(\tilde{R}(\theta, \omega) - R(\theta, \omega) \right)^2 \right] \leq \frac{1}{N} \mathbb{V} \left[\mathbf{p}^t(\mathbf{x})^T \mathbf{1}(g_\omega(f_\theta(\mathbf{x}))) \right] + \mathcal{O} \left(\mathbb{E} [\|\mathbf{p}^t(\mathbf{x}) - \mathbf{p}^*(\mathbf{x})\|_2] \right)^2 \quad (6)$$

where the derivation of Eq. (6) is available in **Appendix C**. On the right-hand side of Eq. (6), the second term dominates when N is large, which suggests that the effectiveness of knowledge distillation is governed by how close the teacher probability $\mathbf{p}^t(\mathbf{x})$ are to the Bayesian probability $\mathbf{p}^*(\mathbf{x})$. The above discussion reached a theoretical guidance 1 for how to integrate the knowledge.

Guidance 1 The instance-level knowledge weights should be set (or learned) in such a way that the integrated teacher probability $\mathbf{p}^t(\mathbf{x})$ is as close as possible to the true Bayesian probability $\mathbf{p}^*(\mathbf{x})$.

(P2) In practice, precisely estimating the squared error to $\mathbf{p}^*(\mathbf{x})$ is not feasible (since $\mathbf{p}^*(\mathbf{x})$ is unknown, especially for those unlabeled data), but one can estimate the quality of the teacher probability $\mathbf{p}^t(\mathbf{x})$ on a holdout set, e.g., by computing the log-loss or squared loss over one-hot labels (Menon et al., 2021). This inspired us to approximately treat $\mathbf{p}^*(\mathbf{x}) \approx \mathbf{e}_y$ on the training set and optimize $\lambda_\gamma(\cdot, \cdot)$ by minimizing the cross-entropy loss $\mathcal{L}_W = \frac{1}{|\mathcal{V}_L|} \sum_{i \in \mathcal{V}_L} \ell(\mathbf{p}^t(\mathbf{x}), \mathbf{p}^*(\mathbf{x}))$. The learned $\lambda_\gamma(\cdot, \cdot)$ is then used to infer the proper teacher probability $\mathbf{p}^t(\mathbf{x}_i)$ for unlabeled data $v_i \in \mathcal{V}_U$. While such estimations are often imperfect, they help to detect poor teacher probabilities, especially for those unlabeled data. The mean squared errors over one-hot labels on the training and testing sets in Fig. 7 also demonstrate the effectiveness of such estimations when $\mathbf{p}^*(\mathbf{x})$ is unknown in practice.

(P3) Furthermore, we derive the following Theorem 1, a theoretical justification for the advantages of AGSSL under the multi-task learning setting, which theoretically proves that the **optimal** integrated teacher $\mathbf{p}^t(\mathbf{x})$ can monotonically approximate $\mathbf{p}^*(\mathbf{x})$ as the number of teachers K increases.

Theorem 1 Define $\Delta(K) = \min \|\mathbf{p}^t(\mathbf{x}_i) - \mathbf{p}^*(\mathbf{x}_i)\|_2 = \min \left\| \sum_{k=1}^K \lambda_\gamma(k, i) \tilde{\mathbf{h}}_i^{(k)} - \mathbf{p}^*(\mathbf{x}_i) \right\|_2$ with $K (K \geq 1)$ given teachers, then we have (1) $\Delta(K+1) \leq \Delta(K)$, and (2) $\lim_{K \rightarrow \infty} \Delta(K) = 0$.

where the above derivation is available in **Appendix D**. The theorem 1 indicates AGSSL is endowed with the theoretical potential to benefit from more teachers, i.e., it has advantages in handling the task-level compatibility, which is also supported by the experimental results in Sec. 4.3 and Fig. 8.

3.3 PARAMETERIZED KNOWLEDGE INTEGRATION

The most common schemes for integrating different levels of knowledge from multiple teachers are averaged assignment (Average) or weighted integration based on labeled data (Weighted). However, averaged assignment fails to differentiate important teachers from irrelevant ones, and the weighted integration may mislead the student in the presence of low-quality teachers. An intuitive illustration of this issue is provided in Fig. 4, where the integrated teacher probability $\mathbf{p}^t(\mathbf{x})$ obtained by the averaged and weighted schemes not only does not come close but even deviates from the true Bayesian probability $\mathbf{p}^*(\mathbf{x})$. Compared to the above two heuristic schemes, this paper aims to adaptively learn the knowledge integration weights by a parameterized weighting function $\lambda_\gamma(\cdot, \cdot)$.

A natural solution to achieve localized knowledge integration is to introduce a weighting function $\lambda_\gamma(\cdot | \gamma_i)$ parameterized by $\gamma_i \in \mathbb{R}^F$. However, directly fitting each $\lambda_\gamma(\cdot | \gamma_i)$ ($1 \leq i \leq N$) locally

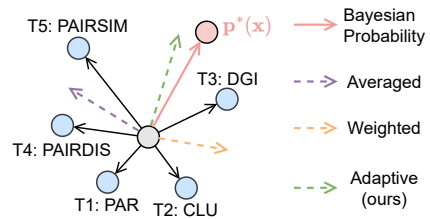


Figure 4: Illustration of the (2D) teacher probability directions for three schemes.

involves solving NF parameters, which increases the over-fitting risk given the limited labels in the graph. Thus, we consider the amortization inference (Kingma & Welling, 2013) which avoids the optimization of parameter γ_i for each node locally and instead fits a shared neural network. In this section, we introduce two schemes, AGSSL-LF and AGSSL-TS, to parameterize the weighting function $\lambda_\gamma(\cdot, \cdot)$, resulting in two specific instantiations of our proposed AGSSL framework.

AGSSL-LF. To explicitly capture the localized importance of different teachers, we introduce a set of latent variables $\{\mu_k\}_{k=1}^K$ and associate each teacher with a latent factor $\mu_k \in \mathbb{R}^C$ to represent it. This strategy is inspired by latent factor models commonly applied in the recommender system (Koren, 2008), where each user or item corresponds to one latent factor used to summarize their implicit features. The importance weight of the k -th teacher to node v_i can be calculated as follows

$$\lambda_\gamma(k, i) = \frac{\exp(\zeta_{k,i})}{\sum_{k'=1}^K \exp(\zeta_{k',i})}, \quad \text{where } \zeta_{k,i} = \nu^T(\mu_k \odot g_\omega(f_\theta(\mathcal{G}, i))) \quad (7)$$

where $\nu \in \mathbb{R}^C$ is a global parameter vector to be learned, which determines whether or not the value of each dimension in $(\mu_k \odot g_\omega(f_\theta(\mathcal{G}, i)))$ has a positive effect on the importance score. Larger $\lambda_\gamma(k, i)$ denotes that the knowledge extracted by k -th teacher is more important to node v_i .

AGSSL-TS. Unlike AGSSL-LF, which calculates importance weights based solely on the node embeddings of different teachers, AGSSL-TS takes into account the matching degree of each teacher-student pair to distill the most matched teacher knowledge into the student model. We separately project the node logits of the student $g_\omega(f_\theta(\mathcal{G}, i)) \in \mathbb{R}^C$ and each teacher $g_{\omega^*}(f_{\theta^*}(\mathcal{G}, i)) \in \mathbb{R}^C$ into two subspaces via a linear transformation with the parameter matrix $\mathbf{W} \in \mathbb{R}^{C \times C}$. Then, the importance weight of k -th teacher (e.g., pretext task) to node v_i can be calculated as follows

$$\lambda_\gamma(k, i) = \frac{\exp(\zeta_{k,i})}{\sum_{k'=1}^K \exp(\zeta_{k',i})}, \quad \text{where } \zeta_{k,i} = \left(\mathbf{W}g_\omega(f_\theta(\mathcal{G}, i))\right)^T \left(\mathbf{W}g_{\omega_k^*}(f_{\theta_k^*}(\mathcal{G}, i))\right) \quad (8)$$

The pseudo-code of the proposed AGSSL framework is summarized in Algorithm 1 in Appendix E.

4 EXPERIMENTAL EVALUATION

In this section, we evaluate AGSSL on eight real-world datasets by answering the following five questions. **Q1:** Can AGSSL achieve better performance compared to training with individual tasks? **Q2:** How does AGSSL compare to other leading graph SSL baselines? **Q3:** Can AGSSL learn localized and customized SSL task strategies? **Q4:** Can AGSSL learn high-quality teacher probabilities $\mathbf{p}^t(\mathbf{x})$? **Q5:** How do the performance of AGSSL-LF and AGSSL-TS compare with other heuristics knowledge integration approaches? Can AGSSL consistently benefit from multiple teachers?

Dataset. The effectiveness of the AGSSL framework is evaluated on eight real-world graph datasets, including Cora (Sen et al., 2008), Citeseer (Giles et al., 1998), Pubmed (McCallum et al., 2000), Coauthor-CS, Coauthor-Physics, Amazon-Photo, Amazon-Computers (Shchur et al., 2018), and ogbn-arxiv (Hu et al., 2020). A statistical overview of these eight datasets is placed in Appendix F. Each set of experiments is run five times with different random seeds, and the average accuracy and standard deviation are reported as performance metrics. Due to space limitations, we defer the implementation details and the best hyperparameter settings for each dataset to Appendix G.

Baseline. To evaluate the capability of AGSSL in automated pretext tasks combinatorial search, we followed Jin et al. (2021) to consider five classical tasks (1) PAR (You et al., 2020b), which predicts pseudo-labels from graph partitioning; (2) CLU (You et al., 2020b), which predicts pseudo-labels from K -means clustering on node features; (3) DGI (Velickovic et al., 2019), which maximizes the mutual information between graph and node representations; (4) PAIRDIS (Jin et al., 2020), which predicts the shortest path length between nodes; and (5) PAIRSIM (Jin et al., 2020), which predicts the feature similarity between nodes. The detailed methodologies for the above five pretext tasks and the reasons why we selected them can be found in Appendix H. In addition to comparing with the automated Graph SSL - AutoSSL (Jin et al., 2021), we also compare AGSSL with some of the state-of-the-art self-supervised baselines in Table 2, including GMI (Peng et al., 2020), MVGRL (Hassani & Khasahmadi, 2020), GRACE (Zhu et al., 2020a), GCA (Zhu et al., 2020b), CG3 (Wan et al., 2020), and BGRL (Thakoor et al., 2021). Note that (1) there is no conflict at all between Graph SSL automation and designing more powerful pretext tasks; and (2) as a general framework, AGSSL is applicable to other more complex self-supervised tasks, which will be left for future work.

Table 1: Performance comparison of single- and multi-task learning, where **bold** and underline denote the best metrics in multi- and single-task learning. Besides, we mark those metrics in multi-task learning that are poorer to vanilla GCNs and (the best) single-task learning as **red** and **blue**.

| Dataset | Setting | GCNs | Single Self-Supervised Task Learning | | | | | Multi Self-Supervised Task Learning | | | |
|------------------------|---------|------------------|--------------------------------------|-------------------------|-------------------------|-------------------------|-------------------------|-------------------------------------|-------------------------|-------------------------|-------------------------|
| | | | PAR | CLU | DGI | PAIRDIS | PAIRSIM | Vanilla | AutoSSL | AGSSL-LF | AGSSL-TS |
| Cora | JT | 81.72 \pm 0.52 | <u>83.52</u> \pm 0.39 | 82.34 \pm 0.46 | 83.28 \pm 0.33 | 82.92 \pm 0.41 | 83.16 \pm 0.38 | 81.50 \pm 0.40 | 83.78 \pm 0.45 | 84.68 \pm 0.39 | 85.32 \pm 0.32 |
| | P&F | 81.72 \pm 0.52 | 82.38 \pm 0.31 | 81.42 \pm 0.35 | 82.10 \pm 0.44 | 81.92 \pm 0.42 | <u>82.44</u> \pm 0.36 | 80.74 \pm 0.38 | 82.96 \pm 0.43 | 84.22 \pm 0.28 | 84.38 \pm 0.27 |
| Citeseer | JT | 71.48 \pm 0.46 | 72.72 \pm 0.36 | 72.14 \pm 0.50 | 73.08 \pm 0.45 | <u>73.16</u> \pm 0.42 | 72.90 \pm 0.45 | <u>72.30</u> \pm 0.50 | 73.30 \pm 0.37 | 74.34 \pm 0.31 | 74.20 \pm 0.42 |
| | P&F | 71.48 \pm 0.46 | 72.36 \pm 0.58 | 71.84 \pm 0.49 | <u>72.52</u> \pm 0.37 | 72.22 \pm 0.53 | 71.98 \pm 0.62 | 71.64 \pm 0.49 | 72.76 \pm 0.44 | 73.58 \pm 0.56 | 73.70 \pm 0.76 |
| Pubmed | JT | 79.26 \pm 0.40 | <u>82.16</u> \pm 0.54 | 80.92 \pm 0.36 | 81.50 \pm 0.43 | 81.22 \pm 0.55 | 80.50 \pm 0.54 | 80.86 \pm 0.50 | 82.72 \pm 0.35 | 82.66 \pm 0.32 | 82.82 \pm 0.29 |
| | P&F | 79.26 \pm 0.40 | 79.56 \pm 0.39 | 79.12 \pm 0.47 | <u>79.90</u> \pm 0.52 | 79.64 \pm 0.48 | 79.34 \pm 0.60 | 78.90 \pm 0.54 | 80.14 \pm 0.41 | 80.62 \pm 0.25 | 80.54 \pm 0.42 |
| CS | JT | 91.04 \pm 0.45 | 92.30 \pm 0.67 | 92.94 \pm 0.70 | 92.66 \pm 0.69 | 92.48 \pm 0.55 | <u>93.12</u> \pm 0.64 | <u>92.16</u> \pm 0.60 | 93.54 \pm 0.46 | 93.86 \pm 0.36 | 93.46 \pm 0.25 |
| | P&F | 91.04 \pm 0.45 | 91.28 \pm 0.55 | 91.36 \pm 0.63 | <u>91.80</u> \pm 0.73 | 91.44 \pm 0.49 | 91.62 \pm 0.47 | <u>91.42</u> \pm 0.57 | 92.48 \pm 0.45 | 92.36 \pm 0.45 | 91.94 \pm 0.33 |
| Physics | JT | 93.06 \pm 0.55 | 94.08 \pm 0.56 | 94.12 \pm 0.49 | <u>94.74</u> \pm 0.46 | 94.62 \pm 0.63 | 94.40 \pm 0.48 | <u>93.94</u> \pm 0.47 | 95.10 \pm 0.42 | 95.74 \pm 0.38 | 95.54 \pm 0.35 |
| | P&F | 93.06 \pm 0.55 | 93.18 \pm 0.71 | 93.50 \pm 0.53 | 93.92 \pm 0.60 | <u>94.04</u> \pm 0.56 | 93.34 \pm 0.73 | <u>93.40</u> \pm 0.50 | 93.88 \pm 0.45 | 94.80 \pm 0.29 | 94.96 \pm 0.43 |
| Photo | JT | 91.90 \pm 0.46 | 92.54 \pm 0.60 | <u>93.04</u> \pm 0.55 | 92.46 \pm 0.70 | 92.32 \pm 0.55 | 92.82 \pm 0.78 | <u>91.52</u> \pm 0.61 | <u>92.94</u> \pm 0.40 | 93.98 \pm 0.29 | 94.22 \pm 0.31 |
| | P&F | 91.90 \pm 0.46 | 92.24 \pm 0.49 | <u>92.58</u> \pm 0.66 | 92.02 \pm 0.59 | 92.10 \pm 0.52 | 92.42 \pm 0.44 | 90.84 \pm 0.51 | <u>92.36</u> \pm 0.45 | 93.32 \pm 0.37 | 93.52 \pm 0.41 |
| Computers | JT | 86.36 \pm 0.65 | 87.48 \pm 0.65 | 87.96 \pm 0.72 | 88.08 \pm 0.64 | 87.62 \pm 0.52 | <u>88.40</u> \pm 0.72 | 86.58 \pm 0.50 | 88.72 \pm 0.44 | 89.56 \pm 0.34 | 89.72 \pm 0.28 |
| | P&F | 86.36 \pm 0.65 | 86.72 \pm 0.78 | <u>87.74</u> \pm 0.80 | 87.36 \pm 0.73 | 86.52 \pm 0.65 | 87.20 \pm 0.69 | 85.90 \pm 0.57 | 88.00 \pm 0.49 | 88.00 \pm 0.42 | 88.00 \pm 0.42 |
| ogbn-arxiv | JT | 71.16 \pm 0.32 | 71.84 \pm 0.28 | 71.72 \pm 0.40 | 72.04 \pm 0.25 | <u>72.18</u> \pm 0.30 | 71.90 \pm 0.33 | 70.94 \pm 0.33 | 72.26 \pm 0.25 | 72.66 \pm 0.26 | 72.72 \pm 0.22 |
| | P&F | 71.16 \pm 0.32 | 71.78 \pm 0.37 | 71.54 \pm 0.36 | <u>71.96</u> \pm 0.28 | 71.90 \pm 0.33 | 71.62 \pm 0.29 | 70.56 \pm 0.31 | 72.08 \pm 0.24 | 72.52 \pm 0.31 | 72.60 \pm 0.25 |
| Avg. Rank \downarrow | JT | 9.63 | 6.50 | 6.63 | 5.25 | 6.00 | 5.75 | 9.13 | 2.88 | 1.75 | 1.50 |
| | P&F | 9.13 | 6.63 | 6.88 | 4.88 | 5.88 | 6.00 | 9.13 | 3.25 | 1.88 | 1.38 |

4.1 PERFORMANCE COMPARISON

Performance Comparison with Individual Tasks (Q1). To answer **Q1**, we report the results for individual and multiple self-supervised tasks under two training strategies, i.e., *Joint Training* (JT) and *Pre-train&Fine-tune* (P&F) in Table. 1, from which we can make the following observations: (1) The performance of individual pretext tasks depends heavily on the datasets, and there does not exist an “optimal” task that works for all datasets. (2) Simply averaging over all tasks (Vanilla) may cause a serious task-level compatibility problem, whose performance may not only be inferior to training with individual tasks (marked in **blue**), but even poorer than the vanilla implementation of GCNs (marked in **red**). (3) As an automated SSL approach, AutoSSL performs better than simply averaging over all tasks, but still lags far behind our proposed AGSSL overall on eight datasets.

Performance Comparison with Representative SSL Baselines (Q2). To answer **Q2**, we compare AGSSL with several representative graph self-supervised baselines. As can be seen from the results reported in Table. 2, by combining just a few simple and classical pretext tasks, the resulting performance is comparable to that of several state-of-the-art self-supervised baselines. For example, AGSSL-LF and AGSSL-TS perform better than other compared methods on 5 out of 8 datasets. Note that these results are provided only to demonstrate the power of AGSSL, and we would like to emphasize again that AGSSL is general enough to be combined with any existing graph SSL tasks.

Table 2: Performance comparison with classical self-supervised algorithms under the *Joint Training* setting, where **bold** and underline denote the best and second metrics on each dataset, respectively.

| Method | Cora | Citeseer | Pubmed | CS | Physics | Photo | Computers | ogbn-arxiv | Avg. Rank \downarrow |
|----------|-------------------------|-------------------------|-------------------------|-------------------------|-------------------------|-------------------------|-------------------------|-------------------------|------------------------|
| GCNs | 81.72 \pm 0.52 | 71.48 \pm 0.46 | 79.26 \pm 0.40 | 91.04 \pm 0.45 | 93.06 \pm 0.55 | 91.90 \pm 0.46 | 86.36 \pm 0.65 | 71.16 \pm 0.32 | 9.83 |
| DGI | 83.28 \pm 0.33 | 73.08 \pm 0.45 | 81.50 \pm 0.43 | 92.66 \pm 0.69 | 94.74 \pm 0.46 | 92.46 \pm 0.70 | 88.08 \pm 0.64 | 72.04 \pm 0.25 | 7.50 |
| GMI | 82.94 \pm 0.40 | 73.22 \pm 0.38 | 81.20 \pm 0.35 | 92.76 \pm 0.56 | <i>OOM</i> | 92.74 \pm 0.56 | 88.20 \pm 0.45 | <i>OOM</i> | 7.00 |
| MVGRL | 83.36 \pm 0.43 | 72.66 \pm 0.37 | 81.74 \pm 0.41 | 92.84 \pm 0.39 | <i>OOM</i> | 93.06 \pm 0.45 | 88.36 \pm 0.51 | <i>OOM</i> | 6.33 |
| GRACE | 80.80 \pm 0.38 | 72.24 \pm 0.44 | 79.96 \pm 0.46 | 91.94 \pm 0.37 | 93.64 \pm 0.47 | 91.92 \pm 0.43 | 87.44 \pm 0.49 | <i>OOM</i> | 9.17 |
| GCA | 84.34 \pm 0.45 | 73.72 \pm 0.37 | 81.98 \pm 0.42 | 93.30 \pm 0.42 | 94.78 \pm 0.52 | 93.30 \pm 0.36 | 88.74 \pm 0.37 | <i>OOM</i> | 4.17 |
| CG3 | 83.76 \pm 0.39 | 73.54 \pm 0.40 | 81.58 \pm 0.36 | 93.02 \pm 0.51 | 94.90 \pm 0.39 | 93.68 \pm 0.48 | 88.42 \pm 0.42 | 72.40 \pm 0.24 | 4.83 |
| BGRL | <u>84.82</u> \pm 0.41 | 73.96 \pm 0.35 | 82.20 \pm 0.34 | <u>93.58</u> \pm 0.29 | 95.12 \pm 0.44 | 93.48 \pm 0.51 | 89.08 \pm 0.38 | 72.80 \pm 0.20 | 2.83 |
| AGSSL-LF | 84.68 \pm 0.39 | 74.34 \pm 0.31 | <u>82.66</u> \pm 0.32 | 93.86 \pm 0.36 | 95.74 \pm 0.38 | <u>93.98</u> \pm 0.29 | <u>89.56</u> \pm 0.34 | 72.66 \pm 0.26 | 1.83 |
| AGSSL-TS | 85.32 \pm 0.32 | <u>74.20</u> \pm 0.42 | 82.82 \pm 0.29 | 93.46 \pm 0.25 | <u>95.54</u> \pm 0.35 | 94.22 \pm 0.31 | 89.72 \pm 0.28 | <u>72.72</u> \pm 0.22 | 1.50 |

4.2 EVALUATION ON LOCALIZED SSL TASKS AND LEARNING CURVES

Localized and Customized SSL strategies (Q3). To answer **Q3**, we visualize the average knowledge weights learned by AGSSL-LF and AGSSL-TS at different node degrees on the Citeseer and Coauthor-CS datasets. From the heatmaps shown in Fig. 5, we can make the following observations: (1) The learned weights vary a lot from dataset to dataset. For example, Citeseer can benefit more from pretext tasks - DGI and PAIRDIS, while pretext tasks CLU and PAIRSIM are more beneficial for Coauthor-CS. (2) The knowledge weights learned by AGSSL-LF and

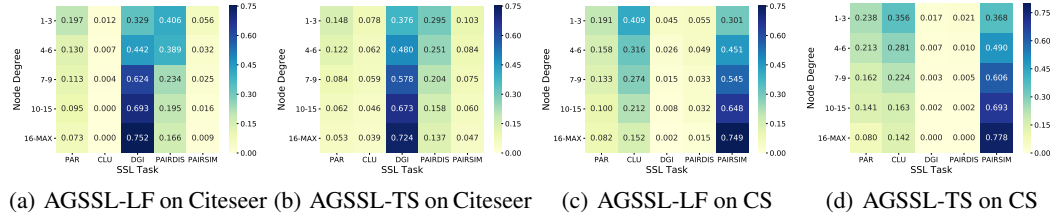


Figure 5: Illustration of average knowledge weights for nodes with different node degree ranges.

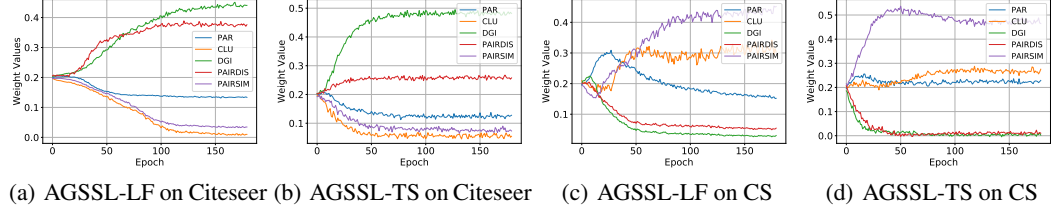


Figure 6: Evolution process of average knowledge weights for nodes with a degree range of [4, 6].

AGSSL-TS are very similar on the same dataset, suggesting that they do uncover some “essence” rather than being completely randomized. (3) The knowledge weights vary greatly across different node degrees, and this variation is almost monotonic. For example, as the node degree increases on Citeseer, the dependence of nodes on DGI increases, while the dependence on PAIRDIS gradually decreases, which indicates that AGSSL has an advantage in learning localized SSL strategies.

Furthermore, we also provide in Fig. 6 the evolution process of knowledge weights for nodes with a degree range of [4, 6] on the Citeseer and Coatuhor-CS datasets. The weights of the five tasks eventually become stable and converge to steady values, corresponding to the results in Fig. 5.

Learning Curves (Q4). Since the true Bayesian probability $\mathbf{p}^*(\mathbf{x})$ is often unknown in practice, it is not feasible to directly estimate the squared errors between $\mathbf{p}^t(\mathbf{x})$ and $\mathbf{p}^*(\mathbf{x})$. Therefore, we follow (Menon et al., 2021; Zhou et al., 2021) to estimate the quality of the teacher probability $\mathbf{p}^t(\mathbf{x})$ by computing the Mean Squared Errors (MSE) over one-hot labels. We provide the curves of MSE and classification accuracy during training in Fig. 7, from which we observe that the MSE gradually decreases while the classification accuracy gradually increases on both the training and testing sets as the training proceeds. This not only demonstrates the effectiveness of the two proposed adaptive knowledge integration methods but also justifies the proposed theoretical guideline 1.

4.3 EVALUATION ON KNOWLEDGE INTEGRATION AND TEACHER NUMBER (Q5)

To answer Q5, we compare AGSSL-LF and AGSSL-TS with three heuristic knowledge integration schemes, including (1) Random, setting $\lambda_\gamma(k, i)$ randomly in the range of [0, 1]; (2) Average, setting $\lambda_\gamma(k, i) = 1/K$ throughout training, and (3) Weighted, calculating cross-entropy as weights on the labeled nodes, and using average weights for unlabeled nodes. For a fair comparison, we perform softmax activation for each scheme to satisfy $\sum_{k=1}^K \lambda_\gamma(k, i) = 1$. We provide the performance of these schemes under five different numbers of teachers in Fig. 8(a) and Fig. 8(b), from which we can see that (1) Random not only does not benefit from multiple teachers but also is poorer than the one trained with one individual task; (2) Average and Weighted cannot always benefit from multiple teachers; for example, the Weighted scheme trained with five pretext task is inferior to the one trained with four pretext tasks on the Citeseer dataset; (3) AGSSL-LF and AGSSL-TS both perform far better than the other three heuristics under various numbers of teachers. More importantly, both AGSSL-LF and AGSSL-TS can consistently benefit from more teachers, which aligns with Theorem 1 and demonstrates the effectiveness of the two proposed knowledge integration strategies.

4.4 EVALUATION ON HYPERPARAMETER SENSITIVITY AND COMPUTATIONAL EFFICIENCY

We provide sensitivity analyses for two hyperparameters, loss weights α and β in Fig. 8(c) and Fig. 8(d), from which it is clear that (1) setting the loss weight α of pretext tasks too large or too small is detrimental to extracting informative knowledge; (2) a large β usually yields good performance,

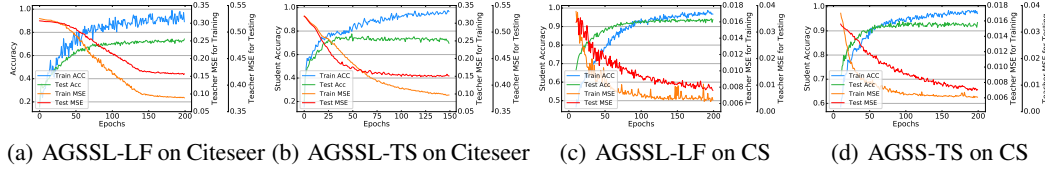


Figure 7: Learning curves of (1) mean squared errors of teacher probability $\mathbf{p}^t(\mathbf{x})$ over the one-hot labels and (2) classification accuracy, to estimate the quality of the teacher probability $\mathbf{p}^t(\mathbf{x})$.

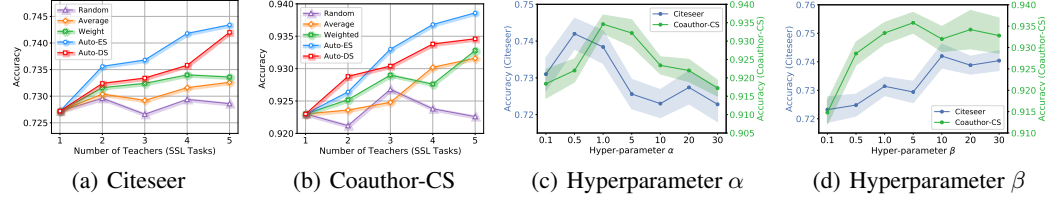


Figure 8: (a-b) Ablation study on knowledge integration under different number of teachers (with concrete values in **Appendix I**). (c-d) Parameter sensitivity analyses on loss weights α and β .

which illustrates the effectiveness of the distillation term in Eq. (4). In practice, we can determine α and β by selecting the model with the highest accuracy on the validation set through the grid search.

Due to space limitation, we place experimental results on **computational efficiency** in **Appendix J**, from which we find that compared to jointly training with multiple pretext tasks, AGSSL not only does not increase, but even has advantages in terms of both training time and peak memory usage.

5 RELATED WORK

Graph Self-supervised Learning (SSL). The primary goal of Graph SSL is to learn transferable prior knowledge from abundant unlabeled data through well-designed pretext tasks. There have been up to hundreds of self-supervised pretext tasks proposed in the past few years, and we refer interested readers to the recent surveys (Wu et al., 2021; Xie et al., 2021; Liu et al., 2021) for more information. Despite the great success, these methods mostly focus on designing more powerful pretext tasks, with little effort to explore how to leverage multiple existing pretext tasks more efficiently.

Automated Machine Learning. One of the most related topics to us is the automated loss function search (Zhao et al., 2021; Weber et al., 2020; Hutter et al., 2019; Waring et al., 2020; Yao et al., 2018). However, most of these methods are specifically designed for image data and may not be applicable for graph-structured data. For example, the loss function of PAIRDIS involves two nodes, which is hardly compatible with the node-specific loss function of CLU. A recent work JOAO (You et al., 2021) on graph contrastive learning is proposed to automatically select data augmentation, but it is tailored for graph classification and single-task contrastive learning and is difficult to extend to multi-task self-supervised learning. Another related work is AUX-TS (Han et al., 2021), which adaptively combines different auxiliary tasks in order to generalize to other tasks during the fine-tuning stage of transfer learning, which is hard to extend directly to the self-supervised setting. The closest work to us is AutoSSL (Jin et al., 2021), which has been discussed in detail in Sec. 2.

6 CONCLUSION

Over the past few years, there have been hundreds of self-supervised algorithms proposed, which inspired us to move our attention away from designing more powerful but complex pretext tasks and towards making more effective use of those already on hand. In this paper, we propose a novel multi-teacher knowledge distillation framework for **Automated Graph Self-Supervised Learning (AGSSL)** to automatically, adaptively, and dynamically learn instance-level self-supervised learning strategies for each node separately. More importantly, we provide a provable theoretical guideline and two adaptive integration strategies to integrate the knowledge from different teachers. While AGSSL automates the selection of pretext tasks for each node, it is still preliminary work, as how to construct a suitable pool of pretext tasks still requires human labor. In this sense, “full” automation is still desired and needs to be pursued in the future. Meanwhile, despite being developed for Graph SSL, extending AGSSL to other self-supervised tasks for image and text data is also a promising direction.

REFERENCES

- Zhao Chen, Vijay Badrinarayanan, Chen-Yu Lee, and Andrew Rabinovich. Gradnorm: Gradient normalization for adaptive loss balancing in deep multitask networks. In *International conference on machine learning*, pp. 794–803. PMLR, 2018.
- Chelsea Finn, Pieter Abbeel, and Sergey Levine. Model-agnostic meta-learning for fast adaptation of deep networks. In *International conference on machine learning*, pp. 1126–1135. PMLR, 2017.
- C Lee Giles, Kurt D Bollacker, and Steve Lawrence. Citeseer: An automatic citation indexing system. In *Proceedings of the third ACM conference on Digital libraries*, pp. 89–98, 1998.
- Michael Gutmann and Aapo Hyvärinen. Noise-contrastive estimation: A new estimation principle for unnormalized statistical models. In *Proceedings of the Thirteenth International Conference on Artificial Intelligence and Statistics*, pp. 297–304. JMLR Workshop and Conference Proceedings, 2010.
- William L Hamilton, Rex Ying, and Jure Leskovec. Inductive representation learning on large graphs. *arXiv preprint arXiv:1706.02216*, 2017.
- Xueting Han, Zhenhuan Huang, Bang An, and Jing Bai. Adaptive transfer learning on graph neural networks. In *Proceedings of the 27th ACM SIGKDD Conference on Knowledge Discovery & Data Mining*, pp. 565–574, 2021.
- Kaveh Hassani and Amir Hosein Khasahmadi. Contrastive multi-view representation learning on graphs. In *International Conference on Machine Learning*, pp. 4116–4126. PMLR, 2020.
- Geoffrey Hinton, Oriol Vinyals, Jeff Dean, et al. Distilling the knowledge in a neural network. *arXiv preprint arXiv:1503.02531*, 2(7), 2015.
- Weihua Hu, Bowen Liu, Joseph Gomes, Marinka Zitnik, Percy Liang, Vijay Pande, and Jure Leskovec. Strategies for pre-training graph neural networks. *arXiv preprint arXiv:1905.12265*, 2019.
- Weihua Hu, Matthias Fey, Marinka Zitnik, Yuxiao Dong, Hongyu Ren, Bowen Liu, Michele Catasta, and Jure Leskovec. Open graph benchmark: Datasets for machine learning on graphs. *arXiv preprint arXiv:2005.00687*, 2020.
- Frank Hutter, Lars Kotthoff, and Joaquin Vanschoren. *Automated machine learning: methods, systems, challenges*. Springer Nature, 2019.
- Wei Jin, Tyler Derr, Haochen Liu, Yiqi Wang, Suhang Wang, Zitao Liu, and Jiliang Tang. Self-supervised learning on graphs: Deep insights and new direction. *arXiv preprint arXiv:2006.10141*, 2020.
- Wei Jin, Xiaorui Liu, Xiangyu Zhao, Yao Ma, Neil Shah, and Jiliang Tang. Automated self-supervised learning for graphs. *arXiv preprint arXiv:2106.05470*, 2021.
- George Karypis and Vipin Kumar. A fast and high quality multilevel scheme for partitioning irregular graphs. *SIAM Journal on scientific Computing*, 20(1):359–392, 1998.
- Alex Kendall, Yarin Gal, and Roberto Cipolla. Multi-task learning using uncertainty to weigh losses for scene geometry and semantics. In *Proceedings of the IEEE conference on computer vision and pattern recognition*, pp. 7482–7491, 2018.
- Diederik P Kingma and Max Welling. Auto-encoding variational bayes. *arXiv preprint arXiv:1312.6114*, 2013.
- Thomas N Kipf and Max Welling. Semi-supervised classification with graph convolutional networks. *arXiv preprint arXiv:1609.02907*, 2016.
- Yehuda Koren. Factorization meets the neighborhood: a multifaceted collaborative filtering model. In *Proceedings of the 14th ACM SIGKDD international conference on Knowledge discovery and data mining*, pp. 426–434, 2008.

- Yixin Liu, Shirui Pan, Ming Jin, Chuan Zhou, Feng Xia, and Philip S Yu. Graph self-supervised learning: A survey. *arXiv preprint arXiv:2103.00111*, 2021.
- Yi Luo, Aiguo Chen, Ke Yan, and Ling Tian. Distilling self-knowledge from contrastive links to classify graph nodes without passing messages. *arXiv preprint arXiv:2106.08541*, 2021.
- J MacQueen. Some methods for classification and analysis of multivariate observations. In *Proc. 5th Berkeley Symposium on Math., Stat., and Prob.*, pp. 281, 1965.
- Andreas Maurer and Massimiliano Pontil. Empirical bernstein bounds and sample variance penalization. *arXiv preprint arXiv:0907.3740*, 2009.
- Andrew Kachites McCallum, Kamal Nigam, Jason Rennie, and Kristie Seymore. Automating the construction of internet portals with machine learning. *Information Retrieval*, 3(2):127–163, 2000.
- Aditya K Menon, Ankit Singh Rawat, Sashank Reddi, Seungyeon Kim, and Sanjiv Kumar. A statistical perspective on distillation. In *International Conference on Machine Learning*, pp. 7632–7642. PMLR, 2021.
- Zhen Peng, Wenbing Huang, Minnan Luo, Qinghua Zheng, Yu Rong, Tingyang Xu, and Junzhou Huang. Graph representation learning via graphical mutual information maximization. In *Proceedings of The Web Conference 2020*, pp. 259–270, 2020.
- Prithviraj Sen, Galileo Namata, Mustafa Bilgic, Lise Getoor, Brian Galligher, and Tina Eliassi-Rad. Collective classification in network data. *AI magazine*, 29(3):93–93, 2008.
- Oleksandr Shchur, Maximilian Mumme, Aleksandar Bojchevski, and Stephan Günnemann. Pitfalls of graph neural network evaluation. *arXiv preprint arXiv:1811.05868*, 2018.
- J Michael Steele. *The Cauchy-Schwarz master class: an introduction to the art of mathematical inequalities*. Cambridge University Press, 2004.
- Fan-Yun Sun, Jordan Hoffmann, Vikas Verma, and Jian Tang. Infograph: Unsupervised and semi-supervised graph-level representation learning via mutual information maximization. *arXiv preprint arXiv:1908.01000*, 2019.
- Shantanu Thakoor, Corentin Tallec, Mohammad Gheshlaghi Azar, Rémi Munos, Petar Veličković, and Michal Valko. Bootstrapped representation learning on graphs. *arXiv preprint arXiv:2102.06514*, 2021.
- Petar Veličković, Guillem Cucurull, Arantxa Casanova, Adriana Romero, Pietro Lio, and Yoshua Bengio. Graph attention networks. *arXiv preprint arXiv:1710.10903*, 2017.
- Petar Velickovic, William Fedus, William L Hamilton, Pietro Liò, Yoshua Bengio, and R Devon Hjelm. Deep graph infomax. In *ICLR (Poster)*, 2019.
- Sheng Wan, Shirui Pan, Jian Yang, and Chen Gong. Contrastive and generative graph convolutional networks for graph-based semi-supervised learning. *arXiv preprint arXiv:2009.07111*, 2020.
- Minjie Wang, Da Zheng, Zihao Ye, Quan Gan, Mufei Li, Xiang Song, Jinjing Zhou, Chao Ma, Lingfan Yu, Yu Gai, Tong He, George Karypis, Jinyang Li, and Zheng Zhang. Deep graph library: A graph-centric, highly-performant package for graph neural networks. *arXiv preprint arXiv:1909.01315*, 2019.
- Jonathan Waring, Charlotta Lindvall, and Renato Umeton. Automated machine learning: Review of the state-of-the-art and opportunities for healthcare. *Artificial intelligence in medicine*, 104: 101822, 2020.
- Michael Weber, Michael Fürst, and J Marius Zöllner. Automated focal loss for image based object detection. In *2020 IEEE Intelligent Vehicles Symposium (IV)*, pp. 1423–1429. IEEE, 2020.
- Lirong Wu, Haitao Lin, Zhangyang Gao, Cheng Tan, Stan Li, et al. Self-supervised on graphs: Contrastive, generative, or predictive. *arXiv preprint arXiv:2105.07342*, 2021.

- Lirong Wu, Zicheng Liu, Jun Xia, Zelin Zang, Siyuan Li, and Stan Z Li. Generalized clustering and multi-manifold learning with geometric structure preservation. In *Proceedings of the IEEE/CVF Winter Conference on Applications of Computer Vision*, pp. 139–147, 2022a.
- Lirong Wu, Lifan Yuan, Guojian Zhao, Haitao Lin, and Stan Z Li. Deep clustering and visualization for end-to-end high-dimensional data analysis. *IEEE Transactions on Neural Networks and Learning Systems*, 2022b.
- Zonghan Wu, Shirui Pan, Fengwen Chen, Guodong Long, Chengqi Zhang, and S Yu Philip. A comprehensive survey on graph neural networks. *IEEE transactions on neural networks and learning systems*, 2020.
- Jun Xia, Lirong Wu, Jintao Chen, Ge Wang, and Stan Z Li. Debaised graph contrastive learning. *arXiv preprint arXiv:2110.02027*, 2021.
- Jun Xia, Lirong Wu, Jintao Chen, Bozhen Hu, and Stan Z Li. Simgrace: A simple framework for graph contrastive learning without data augmentation. In *Proceedings of the ACM Web Conference 2022*, pp. 1070–1079, 2022.
- Yaochen Xie, Zhao Xu, Zhengyang Wang, and Shuiwang Ji. Self-supervised learning of graph neural networks: A unified review. *arXiv preprint arXiv:2102.10757*, 2021.
- Quanming Yao, Mengshuo Wang, Yuqiang Chen, Wenyuan Dai, Yu-Feng Li, Wei-Wei Tu, Qiang Yang, and Yang Yu. Taking human out of learning applications: A survey on automated machine learning. *arXiv preprint arXiv:1810.13306*, 2018.
- Yuning You, Tianlong Chen, Yongduo Sui, Ting Chen, Zhangyang Wang, and Yang Shen. Graph contrastive learning with augmentations. *Advances in Neural Information Processing Systems*, 33, 2020a.
- Yuning You, Tianlong Chen, Zhangyang Wang, and Yang Shen. When does self-supervision help graph convolutional networks? In *International Conference on Machine Learning*, pp. 10871–10880. PMLR, 2020b.
- Yuning You, Tianlong Chen, Yang Shen, and Zhangyang Wang. Graph contrastive learning automated. In *International Conference on Machine Learning*, pp. 12121–12132. PMLR, 2021.
- Hanlin Zhang, Shuai Lin, Weiyang Liu, Pan Zhou, Jian Tang, Xiaodan Liang, and Eric P Xing. Iterative graph self-distillation. *arXiv preprint arXiv:2010.12609*, 2020.
- Shichang Zhang, Yozen Liu, Yizhou Sun, and Neil Shah. Graph-less neural networks: Teaching old mlps new tricks via distillation. *arXiv preprint arXiv:2110.08727*, 2021.
- Xiangyu Zhao, Haochen Liu, Wenqi Fan, Hui Liu, Jiliang Tang, and Chong Wang. Autoloss: Automated loss function search in recommendations. In *Proceedings of the 27th ACM SIGKDD Conference on Knowledge Discovery & Data Mining*, pp. 3959–3967, 2021.
- Helong Zhou, Liangchen Song, Jiajie Chen, Ye Zhou, Guoli Wang, Junsong Yuan, and Qian Zhang. Rethinking soft labels for knowledge distillation: A bias-variance tradeoff perspective. *arXiv preprint arXiv:2102.00650*, 2021.
- Yanqiao Zhu, Yichen Xu, Feng Yu, Qiang Liu, Shu Wu, and Liang Wang. Deep graph contrastive representation learning. *arXiv preprint arXiv:2006.04131*, 2020a.
- Yanqiao Zhu, Yichen Xu, Feng Yu, Qiang Liu, Shu Wu, and Liang Wang. Graph contrastive learning with adaptive augmentation. *arXiv preprint arXiv:2010.14945*, 2020b.
- Daniel Zügner and Stephan Günnemann. Adversarial attacks on graph neural networks via meta learning. *arXiv preprint arXiv:1902.08412*, 2019.

APPENDIX

A. EXTENSIONS TO THE *Pre-train&Fine-tune* (P & F) SETTINGA.1 AUTOSSL FOR THE *Pre-train&Fine-tune* SETTING

To adapt AutoSSL to the *Pre-train&Fine-tune* setting, the learning objective can be formulated as

$$\theta^*, \omega^* = \arg \min_{\theta, \omega} \mathcal{L}_{\text{task}}(\theta_{\text{init}}, \omega) \quad (\text{A.1})$$

where the initialized parameter θ_{init} is obtained by optimizing the following objective function

$$\min_{\{\lambda_k\}_{k=1}^K} \mathcal{H}(f_{\theta_{\text{init}}}(\mathcal{G})), \quad \text{s.t. } \theta_{\text{init}}, \{\eta_k^*\}_{k=1}^K = \arg \min_{\theta, \{\eta_k\}_{k=1}^K} \sum_{k=1}^K \lambda_k \mathcal{L}_{\text{ssl}}^{(k)}(\theta, \eta_k) \quad (\text{A.2})$$

A.2 PROPOSED AGSSL FOR THE *Pre-train&Fine-tune* SETTING

To adapt AGSSL to the *Pre-train&Fine-tune* setting, the learning objective is defined as

$$\min_{\theta, \omega, \gamma} \mathcal{L}_{\text{task}}(\theta, \omega) + \beta \frac{\tau^2}{N} \sum_{i=1}^N \mathcal{L}_{KL} \left(\text{softmax}(\mathbf{z}_i / \tau), \sum_{k=1}^K \lambda_\gamma(k, i) \text{softmax}(\mathbf{h}_i^{(k)} / \tau) \right) \quad (\text{A.3})$$

where $\mathbf{z}_i = g_\omega(f_\theta(\mathcal{G}, i))$ is the logit of node v_i in the student model and $\mathbf{h}_i^{(k)} = g_{\omega_k^*}(f_{\theta_k^*}(\mathcal{G}, i))$ is the logit of node v_i in the k -th teacher model. $\lambda_\gamma(k, i)$ is a parameterized module that outputs the importance weight of k -th pretext task for node v_i , which satisfies $\sum_{k=1}^K \lambda_\gamma(k, i) = 1$. The parameters $\{\theta_k^*\}_{k=1}^K$ and $\{\omega_k^*\}_{k=1}^K$ are obtained by optimizing the following objective function

$$\theta_k^*, \omega_k^* = \arg \min_{(\theta_k, \omega_k)} \mathcal{L}_{\text{task}}(\theta_k^{\text{init}}, \omega_k), \quad \text{s.t. } \theta_k^{\text{init}}, \eta_k^* = \arg \min_{\theta_k, \eta_k} \mathcal{L}_{\text{ssl}}^{(k)}(\theta_k, \eta_k) \quad (\text{A.4})$$

B. DISTILLATION OBJECTIVE REWRITING

Given $\tilde{\mathbf{z}}_i = \text{softmax}(\mathbf{z}_i / \tau)$, $\tilde{\mathbf{h}}_i^{(k)} = \text{softmax}(\mathbf{h}_i^{(k)} / \tau)$, and $\mathbf{p}^t(\mathbf{x}_i) = \sum_{k=1}^K \lambda_\gamma(k, i) \tilde{\mathbf{h}}_i^{(k)}$, we derive how to rewrite the second term of Eq. (4), the *distillation objective*, in the form of $\tilde{R}(\theta, \omega)$ in Eq. (5),

$$\begin{aligned} & \frac{1}{N} \sum_{i=1}^N \mathcal{L}_{KL} \left(\text{softmax}(\mathbf{z}_i / \tau), \sum_{k=1}^K \lambda_\gamma(k, i) \text{softmax}(\mathbf{h}_i^{(k)} / \tau) \right) \\ &= \frac{1}{N} \sum_{i=1}^N \mathcal{L}_{KL} \left(\tilde{\mathbf{z}}_i, \sum_{k=1}^K \lambda_\gamma(k, i) \tilde{\mathbf{h}}_i^{(k)} \right) = \frac{1}{N} \sum_{i=1}^N \mathcal{L}_{KL} \left(\tilde{\mathbf{z}}_i, \mathbf{p}^t(\mathbf{x}_i) \right) \\ &= \frac{1}{N} \sum_{i=1}^N \mathbf{p}^t(\mathbf{x}_i) \log \frac{\mathbf{p}^t(\mathbf{x}_i)}{\tilde{\mathbf{z}}_i} = \frac{1}{N} \sum_{i=1}^N \mathcal{I}(\mathbf{p}^t(\mathbf{x}_i)) - \mathbf{p}^t(\mathbf{x}_i) \log \tilde{\mathbf{z}}_i \end{aligned} \quad (\text{A.5})$$

where $\mathcal{I}(\cdot)$ denotes the information entropy, and since $\mathbf{p}^t(\mathbf{x}_i)$ is fixed during training, we can directly omit the term $\mathcal{L}(\mathbf{p}^t(\mathbf{x}_i))$ and derive the following proportional equation, as follows

$$\frac{1}{N} \sum_{i=1}^N \mathcal{L}(\mathbf{p}^t(\mathbf{x}_i)) - \mathbf{p}^t(\mathbf{x}_i) \log \tilde{\mathbf{z}}_i \propto \frac{1}{N} \sum_{i=1}^N -\mathbf{p}^t(\mathbf{x}_i) \log \tilde{\mathbf{z}}_i = \frac{1}{N} \sum_{i=1}^N \mathbf{p}^t(\mathbf{x}_i) \mathbf{l}(g_\omega(f_\theta(\mathbf{x}_i))) \doteq \tilde{R}(\theta, \omega)$$

where $\mathbf{l}(g_\omega(f_\theta(\mathbf{x}_i))) = (\ell(1, \tilde{\mathbf{z}}_i), \ell(2, \tilde{\mathbf{z}}_i), \dots, \ell(C, \tilde{\mathbf{z}}_i))$ denotes the cross-entropy loss vector, and we have $\tilde{\mathbf{z}}_i = \text{softmax}(\mathbf{z}_i / \tau) = \text{softmax}(g_\omega(f_\theta(\mathbf{x}_i)) / \tau)$.

C. PROOF ON PROPOSITION 1

Proposition 1 Consider an interagted teacher $\mathbf{p}^t(\mathbf{x})$ and a Bayesian teacher $\mathbf{p}^*(\mathbf{x})$. For any GNN encoder $f_\theta(\cdot)$ and prediction head $g_\omega(\cdot)$, the difference between the distillation objective $\tilde{R}(\theta, \omega)$ and Bayesian objective $R(\theta, \omega)$ is bounded by the Mean Square Error (MSE) of their probabilities,

$$\mathbb{E} \left[\left(\tilde{R}(\theta, \omega) - R(\theta, \omega) \right)^2 \right] \leq \frac{1}{N} \mathbb{V} \left[\mathbf{p}^t(\mathbf{x})^t \mathbf{l}(g_\omega(f_\theta(\mathbf{x}))) \right] + \mathcal{O} \left(\mathbb{E} [\| \mathbf{p}^t(x) - \mathbf{p}^*(x) \|_2]^2 \right) \quad (\text{A.6})$$

Proof 1 Let us start the derivation from the left side of the equation, as follows

$$\mathbb{E} \left[\left(\tilde{R}(\theta, \omega) - R(\theta, \omega) \right)^2 \right] = \mathbb{V} \left[\left(\tilde{R}(\theta, \omega) - R(\theta, \omega) \right) \right] + \mathbb{E} \left[\left(\tilde{R}(\theta, \omega) - R(\theta, \omega) \right) \right]^2 \quad (\text{A.7})$$

Since $R(\theta, \omega)$ can be considered as a constant in practice, we have

$$\begin{aligned} \mathbb{V} \left[\left(\tilde{R}(\theta, \omega) - R(\theta, \omega) \right) \right] &= \mathbb{V} \left[\tilde{R}(\theta, \omega) \right] + \mathbb{V} [R(\theta, \omega)] - \text{Cov} \left(\tilde{R}(\theta, \omega), R(\theta, \omega) \right) \\ &= \mathbb{V} \left[\tilde{R}(\theta, \omega) \right] = \frac{1}{N} \mathbb{V} \left[\mathbf{p}^t(\mathbf{x})^t \mathbf{l}(g_\omega(f_\theta(\mathbf{x}))) \right] \end{aligned} \quad (\text{A.8})$$

Next, we consider the second term on the right-hand side in Eq. (A.7), as follows

$$\begin{aligned} \mathbb{E} \left[\left(\tilde{R}(\theta, \omega) - R(\theta, \omega) \right) \right]^2 &= \mathbb{E}_{\mathbf{x}} \left[\mathbf{p}^t(\mathbf{x})^t \mathbf{l}(g_\omega(f_\theta(\mathbf{x}))) - \mathbf{p}^*(\mathbf{x})^t \mathbf{l}(g_\omega(f_\theta(\mathbf{x}))) \right]^2 \\ &= \mathbb{E}_{\mathbf{x}} \left[\left(\mathbf{p}^t(\mathbf{x})^t - \mathbf{p}^*(\mathbf{x})^t \right) \mathbf{l}(g_\omega(f_\theta(\mathbf{x}))) \right]^2 \\ &\leq \mathbb{E}_{\mathbf{x}} \left[\left\| \mathbf{p}^t(\mathbf{x})^t - \mathbf{p}^*(\mathbf{x})^t \right\|_2 \cdot \left\| \mathbf{l}(g_\omega(f_\theta(\mathbf{x}))) \right\|_2 \right]^2 \\ &\doteq \mathcal{O} \left(\mathbb{E} \left[\left\| \mathbf{p}^t(x) - \mathbf{p}^*(x) \right\|_2 \right] \right)^2 \end{aligned} \quad (\text{A.9})$$

where the inequality holds according to Cauchy-Schwartz inequality (Steele, 2004). Combining the derivations of Eq. (A.8) and Eq. (A.9) into Eq. (A.7), we obtain the final inequality as follows

$$\mathbb{E} \left[\left(\tilde{R}(\theta, \omega) - R(\theta, \omega) \right)^2 \right] \leq \frac{1}{N} \mathbb{V} \left[\mathbf{p}^t(\mathbf{x})^t \mathbf{l}(g_\omega(f_\theta(\mathbf{x}))) \right] + \mathcal{O} \left(\mathbb{E} \left[\left\| \mathbf{p}^t(x) - \mathbf{p}^*(x) \right\|_2 \right] \right)^2 \quad (\text{A.10})$$

D. PROOF ON THEOREM 1

Theorem 1 Define $\Delta(K) = \min \left\| \mathbf{p}^t(\mathbf{x}_i) - \mathbf{p}^*(\mathbf{x}_i) \right\|_2 = \min \left\| \sum_{k=1}^K \lambda_\gamma(k, i) \tilde{\mathbf{h}}_i^{(k)} - \mathbf{p}^*(\mathbf{x}_i) \right\|_2$ with $K (K \geq 1)$ given teachers, then we have (1) $\Delta(K+1) \leq \Delta(K)$, and (2) $\lim_{K \rightarrow \infty} \Delta(K) = 0$.

Proof. Let us simplify the symbol $\lambda_\gamma(k, i)$ to λ_k and consider the case with K teachers, we have

$$\begin{aligned} \{\lambda_k^*\}_{k=1}^K &= \arg \min_{\{\lambda_k\}_{k=1}^K} \left\| \sum_{k=1}^K \lambda_k \tilde{\mathbf{h}}_i^{(k)} - \mathbf{p}^*(x) \right\| \\ \Delta \mathbf{p}_K &= \sum_{k=1}^K \lambda_k^* \tilde{\mathbf{h}}_i^{(k)} - \mathbf{p}^*(x), \Delta(K) = \|\Delta \mathbf{p}_K\|_2 \end{aligned} \quad (\text{A.11})$$

Next, let's consider the case with $(K+1)$ teachers, as follows

$$\begin{aligned} \Delta(K+1) &= \min_{\{\lambda_k\}_{k=1}^{K+1}} \left\| \sum_{k=1}^{K+1} \lambda_k \tilde{\mathbf{h}}_i^{(k)} - \mathbf{p}^*(\mathbf{x}_i) \right\|_2 \\ &\leq \min_{\lambda_{K+1}} \left\| \sum_{k=1}^K \lambda_k^* \tilde{\mathbf{h}}_i^{(k)} + \lambda_{K+1} \tilde{\mathbf{h}}_i^{(K+1)} - \mathbf{p}^*(\mathbf{x}_i) \right\|_2 \\ &= \min_{\lambda_{K+1}} \left\| \lambda_{K+1} \tilde{\mathbf{h}}_i^{(K+1)} + \Delta \mathbf{p}_K \right\|_2 \\ &\leq \sin \left(\arccos \frac{\langle \Delta \mathbf{p}_K, \tilde{\mathbf{h}}_i^{(K+1)} \rangle}{\|\Delta \mathbf{p}_K\|_2 \cdot \|\tilde{\mathbf{h}}_i^{(K+1)}\|_2} \right) \cdot \|\Delta \mathbf{p}_K\|_2 \\ &\leq \|\Delta \mathbf{p}_K\|_2 = \Delta(K) \end{aligned} \quad (\text{A.12})$$

where the equality in the fourth row of Eq. (A.12) holds under the condition that

$$\lambda_{k+1} = - \frac{\langle \Delta \mathbf{p}_K, \tilde{\mathbf{h}}_i^{(K+1)} \rangle}{\|\Delta \mathbf{p}_K\|_2 \cdot \|\tilde{\mathbf{h}}_i^{(K+1)}\|_2} \cdot \frac{\|\Delta \mathbf{p}_K\|_2}{\|\tilde{\mathbf{h}}_i^{(K+1)}\|_2} = - \frac{\langle \Delta \mathbf{p}_K, \tilde{\mathbf{h}}_i^{(K+1)} \rangle}{\|\tilde{\mathbf{h}}_i^{(K+1)}\|_2^2} \quad (\text{A.13})$$

Let $K \geq 2$ be the number of teachers, and the results of the K -th iteration can be defined as follows:

$$\begin{aligned}
\Delta(K) &\leq \sin \left(\arccos \frac{\langle \Delta \mathbf{p}_{K-1}, \tilde{\mathbf{h}}_i^{(K)} \rangle}{\|\Delta \mathbf{p}_{K-1}\|_2 \cdot \|\tilde{\mathbf{h}}_i^{(K)}\|_2} \right) \cdot \Delta(K-1) \\
&\leq \sin \left(\arccos \frac{\langle \Delta \mathbf{p}_{K-1}, \tilde{\mathbf{h}}_i^{(K)} \rangle}{\|\Delta \mathbf{p}_{K-1}\|_2 \cdot \|\tilde{\mathbf{h}}_i^{(K)}\|_2} \right) \cdot \sin \left(\arccos \frac{\langle \Delta \mathbf{p}_{K-2}, \tilde{\mathbf{h}}_i^{(K-1)} \rangle}{\|\Delta \mathbf{p}_{K-2}\|_2 \cdot \|\tilde{\mathbf{h}}_i^{(K-1)}\|_2} \right) \cdot \Delta(K-2) \\
&\leq \dots \\
&\leq \prod_{k=2}^K \sin \left(\arccos \frac{\langle \Delta \mathbf{p}_{k-1}, \tilde{\mathbf{h}}_i^{(k)} \rangle}{\|\Delta \mathbf{p}_{k-1}\|_2 \cdot \|\tilde{\mathbf{h}}_i^{(k)}\|_2} \right) \cdot \Delta(1)
\end{aligned}$$

Since $\sin \left(\arccos \frac{\langle \Delta \mathbf{p}_{k-1}, \tilde{\mathbf{h}}_i^{(k)} \rangle}{\|\Delta \mathbf{p}_{k-1}\|_2 \cdot \|\tilde{\mathbf{h}}_i^{(k)}\|_2} \right) \leq 1$, and the equality holds when and only when $\Delta \mathbf{p}_{k-1}$ and $\tilde{\mathbf{h}}_i^{(k)}$ are orthogonal, which in practice is hard to be satisfied, we have $\lim_{K \rightarrow \infty} \Delta(K) = 0$.

E. PSEUDO CODE OF AGSSL

The pseudo-code of the proposed AGSSL framework is summarized in Algorithm 1.

Algorithm 1 Algorithm for the *Multi-teacher Knowledge Distillation* framework for AGSSL

Input: Graph $\mathcal{G} = (\mathcal{V}, \mathcal{E}, \mathbf{X})$, Number of Pretext Tasks: K , and Number of Epochs: T .

Output: Predicted Labels \mathcal{Y}_U , GNN Encoder $f_\theta(\cdot)$, and Prediction Head $g_\omega(\cdot)$.

- 1: Randomly initialize the parameters of K teacher models and a student model.
 - 2: Pre-train each teacher with one pretext task to get pre-trained parameters $\{\theta_k^*, \omega_k^*\}_{k=1}^K$.
 - 3: **for** $t \in \{0, 1, \dots, T-1\}$ **do**
 - 4: Output logits $\{\mathbf{h}_i^{(k)} = g_{\omega_k^*}(f_{\theta_k^*}(\mathcal{G}, i))\}_{k=1}^K$ from the pre-trained teachers and freeze them.
 - 5: Integrate the knowledge of different teachers by $\mathbf{p}^t(\mathbf{x}_i) = \sum_{k=1}^K \lambda_\gamma(k, i) \text{softmax}(\mathbf{h}_i^{(k)}/\tau)$.
 - 6: Jointly perform distillation by Eq. (4) and optimize the function $\lambda_\gamma(\cdot, \cdot)$ with loss \mathcal{L}_W .
 - 7: **end for**
 - 8: **return** Predicted labels \mathcal{Y}_U , GNN encoder $f_\theta(\cdot)$, and prediction head $g_\omega(\cdot)$.
-

F. DATASET STATISTICS

Eight publicly available graph datasets are used to evaluate the proposed AGSSL framework. An overview summary of the statistical characteristics of datasets is given in Tab. A1. For the three small-scale datasets, namely Cora, Citeseer, and Pubmed, we follow the data splitting strategy in (Kipf & Welling, 2016). For the four large-scale datasets, namely Coauthor-CS, Coauthor-Physics, Amazon-Photo, and Amazon-Computers, we follow (Zhang et al., 2021; Luo et al., 2021) to randomly split the data into train/val/test sets, and each random seed corresponds to a different splitting. For the ogbn-arxiv dataset, we use the public data splits provided by the authors (Hu et al., 2020).

Table A1: Statistical information of the datasets.

| Dataset | Cora | Citeseer | Pubmed | Photo | CS | Physics | Computers | ogbn-arxiv |
|------------|------|----------|--------|--------|-------|---------|-----------|------------|
| # Nodes | 2708 | 3327 | 19717 | 7650 | 18333 | 34493 | 13752 | 169343 |
| # Edges | 5278 | 4614 | 44324 | 119081 | 81894 | 247962 | 245861 | 1166243 |
| # Features | 1433 | 3703 | 500 | 745 | 6805 | 8415 | 767 | 128 |
| # Classes | 7 | 6 | 3 | 8 | 15 | 5 | 10 | 40 |
| Label Rate | 5.2% | 3.6% | 0.3% | 2.1% | 1.6% | 0.3% | 1.5% | 53.7% |

G. HYPERPARAMETER SETTINGS

The following hyperparameters are set the same for all datasets: Adam optimizer with learning rate $lr = 0.01$ (0.001 for ogbn-arxiv) and weight decay $w = 5e-4$; Epoch $E = 500$;

Layer number $L = 1$ (2 for `ogb-arxiv`). The other dataset-specific hyperparameters are determined by an AutoML toolkit NNI with the hyperparameter search spaces as: hidden dimension $F = \{32, 64, 128, 256, 512\}$; distillation temperature $\tau = \{1, 1.2, 1.5, 2, 3, 4, 5\}$, and loss weights $\alpha, \beta = \{0.1, 0.5, 1, 5, 10, 20, 30\}$. For a fairer comparison, the model with the highest validation accuracy is selected for testing. Besides, the best hyperparameter choices for each dataset are available in the supplementary. Moreover, the experiments on both baselines and our approach are implemented based on the standard implementation in the DGL library (Wang et al., 2019) using the PyTorch 1.6.0 with Intel(R) Xeon(R) Gold 6240R @ 2.40GHz CPU and NVIDIA V100 GPU.

H. DETAILS ON FIVE PRETEXT TASKS

In this paper, we evaluate the capability of AGSSL in automatic pretext tasks combinatorial search with five classical pretext tasks, including PAR (You et al., 2020b), CLU (You et al., 2020b), DGI (Velickovic et al., 2019), PAIRDIS (Jin et al., 2020), and PAIRSIM (Jin et al., 2020). Our motivations for selecting these five pretext tasks are 4-fold: (1) *Fair comparison*. To make a fair comparison with previous methods (e.g., AutoSSL), we keep in line with it in the setting of pretext tasks, i.e., using the same combination of tasks. (2) *Simple but classical*. We should pick those pretext tasks that are simple but classical enough, rather than those that are overly complex, not time-tested, and not well known. This is to avoid, whether the resulting performance gains come from our proposed AGSSL or from the complexity of the selected pretext task itself, becoming incomprehensible and hard to explain. (3) *Comprehensive*. Different pretext tasks implicitly involve different inductive biases, so it is important to consider different aspects comprehensively when selecting pretext tasks, rather than picking too many homogeneous and similar tasks. (4) *Applicability*. There is no conflict at all between Graph SSL automation and designing more powerful pretext tasks; as a general framework, AGSSL is applicable to other more complex self-supervised tasks. However, the focus of this paper is on the knowledge distillation framework rather than on the specific task design, and it is also impractical to enumerate and compare all existing graph SSL methods in a limited space.

PAR and CLU. The pretext task of Node Clustering (CLU) pre-assigns a pseudo-label \hat{y}_i , e.g., the cluster index, to each node $v_i \in \mathcal{V}$ by K -means clustering algorithm (MacQueen, 1965). The learning objective of this pretext task is then formulated as a classification problem, as follows

$$\mathcal{L}_{\text{ssl}}(\theta, \eta) = \frac{1}{N} \sum_{v_i \in \mathcal{V}} \ell(g_\eta(f_\theta(\mathcal{G}, i), \hat{y}_i)) \quad (\text{A.14})$$

When node attributes are not available, another choice to obtain pseudo-labels is based on the topology of the graph structure. Specifically, the pretext task of graph partitioning (PAR) predicts partition pseudo-labels obtained by the Metis graph partition (Karypis & Kumar, 1998). The two tasks, CLU and PAR, are very similar, but they extract *feature-level* and *topology-level* knowledge from the graph, respectively. A key hyperparameter of them is the category number of pseudo-labels $\#P$, which is set to $\#P=10$ for CLU and $\#P=400$ (100 for Amazon-Photo and Amazon-Computers, 1000 for Citeseer) for PAR, following the settings in (Jin et al., 2021). In practice, CLU can be easily extended to other variants by adopting other clustering methods (Wu et al., 2022b;a).

DGI. Deep Graph Infomax (DGI) is proposed to contrast the node representations and corresponding high-level summary of graphs. First, it applies an augmentation transformation $\mathcal{T}(\cdot)$ to obtain an augmented graph $\tilde{\mathcal{G}} = \mathcal{T}(\mathcal{G})$. Then a shared graph encoder $f_\theta(\cdot)$ is applied to obtain node embeddings $\mathbf{h}_i = f_\theta(\mathcal{G}, i)$ and $\tilde{\mathbf{h}}_i = f_\theta(\tilde{\mathcal{G}}, i)$. Beside, a global mean pooling is applied to obtain the graph-level representation $\mathbf{h}_{\tilde{\mathcal{G}}} = \frac{1}{N} \sum_{i=1}^N \tilde{\mathbf{h}}_i$. Finally, the learning objective is defined as follows

$$\mathcal{L}_{\text{ssl}}(\theta) = -\frac{1}{N} \sum_{v_i \in \mathcal{V}} \mathcal{MI}(\mathbf{h}_{\tilde{\mathcal{G}}}, \mathbf{h}_i) \quad (\text{A.15})$$

where $\mathcal{MI}(\cdot, \cdot)$ is the InfoNCE mutual information estimator (Gutmann & Hyvärinen, 2010), where the negative samples to contrast with $\mathbf{h}_{\tilde{\mathcal{G}}}$ is $\{\mathbf{h}_j\}_{j \neq i}$. The pretext task of DGI extracts knowledge at the graph level. To improve the computational efficiency for large-scale graphs, we will randomly sample 2000 nodes to contrast the representations between these sampled nodes and the whole graph.

PAIRDIS. The pretext task of PAIRDIS aims to guide the model to preserve *global topology information* by predicting the shortest path length between nodes. It first randomly samples a certain

amount of node pairs \mathcal{S} and calculates the pairwise node shortest path length $d_{i,j} = d(v_i, v_j)$ for node pairs $(v_i, v_j) \in \mathcal{S}$. Furthermore, it groups the shortest path lengths into four categories: $C_{i,j} = 0, C_{i,j} = 1, C_{i,j} = 2$, and $C_{i,j} = 3$ corresponding to $d_{i,j} = 1, d_{i,j} = 2, d_{i,j} = 3$, and $d_{i,j} \geq 4$, respectively. The learning objective can be formulated as a multi-class classification problem,

$$\mathcal{L}_{\text{ssl}}(\theta, \eta) = \frac{1}{|\mathcal{S}|} \sum_{(v_i, v_j) \in \mathcal{S}} \ell(g_\eta(|f_\theta(\mathcal{G})_{v_i} - f_\theta(\mathcal{G})_{v_j}|), C_{i,j}) \quad (\text{A.16})$$

where $\ell(\cdot)$ denotes the cross entropy loss and $g_\eta(\cdot)$ linearly maps the input to a 1-dimension value. A key hyperparameter in PAIRDIS is the size of \mathcal{S} , which is set to $|\mathcal{S}| = 400$ for all eight datasets.

PAIRSIM. Unlike PAIRDIS, which focuses on the global topology, PAIRSIM adopts link prediction as a pretext task to predict feature similarities between node pairs and thus capture **local connectivity information** from the graph. PAIRSIM first masks m edges $\mathcal{M} \in \mathcal{E}$ and also samples m edges $\bar{\mathcal{M}} \in \{(v_i, v_j) | v_i, v_j \in \mathcal{V} \text{ and } (v_i, v_j) \notin \mathcal{E}\}$. Then, the learning objective of PAIRSIM is to predict whether there exists a link between a given node pair, which can be formulated as follows

$$\mathcal{L}_{\text{ssl}}(\theta, \eta) = \frac{1}{2m} \left(\sum_{e_{i,j} \in \mathcal{M}} \ell(g_\eta(|f_\theta(\mathcal{G}, i) - f_\theta(\mathcal{G}, j)|), 1) + \sum_{e_{i,j} \in \bar{\mathcal{M}}} \ell(g_\eta(|f_\theta(\mathcal{G}, i) - f_\theta(\mathcal{G}, j)|), 0) \right)$$

where $\ell(\cdot)$ denotes the cross entropy loss and $g_\eta(\cdot)$ linearly maps the input to a 1-dimension value. The pretext task of PAIRSIM aims to help GNN learn more local structural information. A key hyperparameter in PAIRSIM is the size of \mathcal{M} , which is set to $|\mathcal{M}| = 400$ for all eight datasets.

Table A2: Ablation study on knowledge integration under different number of teachers, where **bold** and underline denote the best and second metrics for each teacher number, respectively. The best performance (i.e., the optimal teacher number) for each integration scheme is marked in **blue**.

| Method | Citeseer | | | | | Coauthor-CS | | | | |
|----------|------------------|----------------------------------|----------------------------------|----------------------------------|----------------------------------|------------------|----------------------------------|----------------------------------|----------------------------------|----------------------------------|
| | 1 (+PAR) | 2 (+CLU) | 3 (+DGI) | 4 (+PAIRDIS) | 5 (+PAIRSIM) | 1 (+PAR) | 2 (+CLU) | 3 (+DGI) | 4 (+PAIRDIS) | 5 (+PAIRSIM) |
| Random | 72.72 \pm 0.36 | 72.96\pm0.47 | 72.66 \pm 0.39 | 72.94 \pm 0.43 | 72.86 \pm 0.45 | 92.30 \pm 0.67 | 92.12 \pm 0.54 | 92.68\pm0.47 | 92.38 \pm 0.53 | 92.26 \pm 0.64 |
| Average | 72.72 \pm 0.36 | 73.04 \pm 0.34 | 72.92 \pm 0.42 | 73.16 \pm 0.39 | 73.26\pm0.37 | 92.30 \pm 0.67 | 92.36 \pm 0.49 | 92.48 \pm 0.60 | 93.02 \pm 0.55 | 93.16\pm0.47 |
| Weighted | 72.72 \pm 0.36 | 73.16 \pm 0.32 | 73.24 \pm 0.46 | 73.40\pm0.43 | 73.36 \pm 0.40 | 92.30 \pm 0.67 | 92.52 \pm 0.46 | 92.90 \pm 0.51 | 92.76 \pm 0.39 | 93.28\pm0.53 |
| AGSSL-LF | 72.72 \pm 0.36 | 73.56\pm0.39 | 73.68\pm0.33 | 74.18\pm0.40 | 74.34\pm0.31 | 92.30 \pm 0.67 | 92.64\pm0.44 | 93.30\pm0.37 | 93.68\pm0.52 | 93.86\pm0.36 |
| AGSSL-TS | 72.72 \pm 0.36 | 73.24\pm0.44 | 73.34\pm0.40 | 73.58\pm0.38 | 74.20\pm0.42 | 92.30 \pm 0.67 | 92.88\pm0.34 | 93.04\pm0.26 | 93.38\pm0.31 | 93.46\pm0.25 |

I. DETAILS ON EXPERIMENTAL RESULTS

Table. A2 provides the concrete values of experimental results in Fig. 8(a) and Fig. 8(b). The setting of different teacher combination is (1) one teacher: PAR; (2) two teachers: PAR and CLU; (3) three teachers: PAR, CLU, and DGI; (4) four teachers: PAR, CLU, DGI, and PAIRDIS; and (5) five teachers: PAR, CLU, DGI, PAIRDIS, and PAIRSIM. As can be seen from Table. A2, AGSSL-LF and AGSSL-TS always perform better than other three heuristic methods; their performance increases consistently with the number of teachers, reaching the best at a number of five teachers.

Table A3: Comparison of the computational resources in terms of training time (s) and peak memory (M) among AGSSL-LF, AGSSL-TS and the *Joint Training* (JOINT-T) on eight graph datasets.

| Method | Resource | Cora | Citeseer | Pubmed | CS | Physics | Photo | Computers | ogbn-arxiv |
|----------|---------------|--------|----------|--------|--------|---------|--------|-----------|------------|
| JOINT-T | Training Time | 17.87s | 18.57s | 75.18s | 98.83s | 171.61s | 36.73s | 51.90s | 1362.28s |
| | Peak Memory | 1527M | 1915M | 7415M | 10235M | 22851M | 4358M | 4478M | 24573M |
| AGSSL-LF | Training Time | 15.42s | 16.09s | 68.31s | 91.76s | 158.73s | 32.61s | 45.96s | 1289.73s |
| | Peak Memory | 1422M | 1618M | 5834M | 6512M | 14395M | 3693M | 3847M | 15739M |
| AGSSL-TS | Training Time | 15.53s | 16.22s | 68.67s | 92.14s | 159.24s | 32.84s | 46.26s | 1294.67s |
| | Peak Memory | 1453M | 1695M | 5912M | 6624M | 14538M | 3752M | 3915M | 15923M |

J. COMPUTATIONAL EFFICIENCY

We compare the training time and peak memory of AGSSL with the joint training (JOINT-T) of multiple pretext tasks with fixed weights in Table. A3. It can be seen that while AGSSL needs to

train multiple teacher models separately, it has advantages over JOINT-T in terms of both training time and peak memory, mainly because: (1) compared to JOINT-T that trains multiple pretext tasks **simultaneously**, each teacher in AGSSL can be trained **sequentially**, which greatly reduces the peak memory usage; (2) the training with multiple tasks is more difficult to optimize than the training with one single task, so **each training epoch of JOINT-T takes longer time** than AGSSL; and (3) JOINT-T is more difficult to converge with higher complexity, i.e., **it requires more training epochs to converge**. Instead, while AGSSL needs to train several more models, it takes much less time for each model, resulting in an overall training time even slightly less than JOINT-T. (4) AGSSL-LF and AGSSL-TS differ only in their knowledge integration schemes, so their overall resource usage (e.g., training time and peak memory) is very close and much less than JOINT-T.